Helmholtz-Zentrum Dresden-Rossendorf (HZDR)

HELMHOLTZ ZENTRUM
DRESDEN ROSSENDORF

# A mineral liberation study of grain boundary fracture based on measurements of the surface exposure after milling

Leißner, T.; Hoang, D.; Rudolph, M.; Heinig, T.; Bachmann, K.; Gutzmer, J.; Schubert, H.; Peuker, U. A.;

Originally published:

August 2016

**International Journal of Mineral Processing 156(2016), 3-13**

DOI: https://doi.org/10.1016/j.minpro.2016.08.014

Perma-Link to Publication Repository of HZDR:

https://www.hzdr.de/publications/Publ-24056

Release of the secondary publication
on the basis of the German Copyright Law § 38 Section 4.

CC BY-NC-ND

Accepted Manuscript

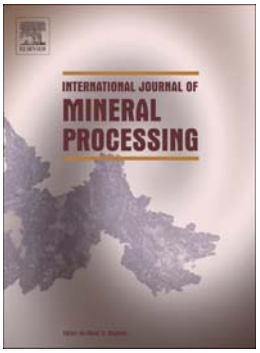


# A mineral liberation study of grain boundary fracture based on measurements of the surface exposure after milling

T. Leißner, D.H. Hoang, M. Rudolph, T. Heinig, K. Bachmann, J. Gutzmer, H. Schubert, U.A. Peuker

PII: S0301-7516(16)30168-5
DOI: doi: 10.1016/j.minpro.2016.08.014
Reference: MINPRO 2946

To appear in: *International Journal of Mineral Processing*

Received date: 30 December 2015
Revised date: 26 August 2016
Accepted date: 30 August 2016

Please cite this article as: Leißner, T., Hoang, D.H., Rudolph, M., Heinig, T., Bachmann, K., Gutzmer, J., Schubert, H., Peuker, U.A., A mineral liberation study of grain boundary fracture based on measurements of the surface exposure after milling, *International Journal of Mineral Processing* (2016), doi: 10.1016/j.minpro.2016.08.014

This is a PDF file of an unedited manuscript that has been accepted for publication. As a service to our customers we are providing this early version of the manuscript. The manuscript will undergo copyediting, typesetting, and review of the resulting proof before it is published in its final form. Please note that during the production process errors may be discovered which could affect the content, and all legal disclaimers that apply to the journal pertain.

ACCEPTED MANUSCRIPT

# A mineral liberation study of grain boundary fracture based on measurements of the surface exposure after milling

T. Leißner[a]; D. H. Hoang[a,b,c]; M. Rudolph[c], T. Heinig[c], K. Bachmann[c], J. Gutzmer[c,d], H. Schubert[a] and U. A. Peuker[a]

[a] Technische Universität Bergakademie Freiberg, Institute of Mechanical Process Engineering and Mineral Processing, Agricolastraße 1, 09599 Freiberg, Germany

[b] Department of Mineral Processing, Faculty of Mining, Hanoi University of Mining and Geology, Duc Thang, Bac Tu Liem, Hanoi, Vietnam

[c] Helmholtz-Zentrum Dresden-Rossendorf, Helmholtz Institute Freiberg for Resource Technology, Chemnitzer Str. 40, 09599 Freiberg, Germany

[d] Technische Universität Bergakademie Freiberg, Department of Mineralogy, Brennhausgasse 14, 09596 Freiberg, Germany

ACCEPTED MANUSCRIPT

## Abstract

Minerals can be liberated by random fracture of particles into smaller fragments or by detachment along phase boundaries. These two mechanisms represent borderline cases. When ores get comminuted the liberation of minerals is achieved to some extent by both mechanisms. This article describes a method to determine the extent of transgranular and intergranular fracture based on 2-dimensional analysis of surface exposure of minerals.

The approach uses the unbiased surface information of phase specific surface area (*PSSA*), phase specific free surface (*PSFS*) and phase specific interfacial area (*PSIA*) of minerals and their change with comminution. The parameters are discussed related to the normalized grain size, which is the ratio of mineral grain size in the product to mineral grain size in the unbroken material. Finally, the amount of transgranular and intergranular fracture on surface exposure can be calculated using the phase specific surface parameters.

A sedimentary rock (apatite ore), an igneous rock (nepheline-syenite) and an artificial material (copper slags) were ground to different fineness. Based on the mineral liberation analysis (MLA) of feed and products, the extent of phase boundary fracture on the surface exposure of the minerals is studied.

## Keywords

Mineral liberation analysis, preferential breakage, transgranular fracture, intergranular fracture, random fracture, grain boundary fracture

ACCEPTED MANUSCRIPT

## 1. Introduction

Mechanisms causing mineral liberation were first described by Gaudin (1939). He distinguished between liberation by comminution and liberation by detachment. The latter represents a fracture along grain boundaries (intergranular fracture). Liberation by comminution is given as a random fracture mechanism which is not being influenced by ore texture, grain boundaries and mineral features (transgranular fracture). As there is no general definition for random fracture different wording and various definitions can be found in literature. Recently Mariano and coworkers (2016) summarized the definitions of random fracture used by different authors. The article highlighted “the absence of methods to measure the relative distributions of random and non-random breakage to liberation” (Mariano et al., 2016).

Random fracture is often accounted for as the dominating mechanism for the liberation of ore minerals. It therefore had been a basis to simplify models for liberation modelling (Barbery, 1991, 1992; King, 1979; Meloy, 1984). Meloy (1984) postulated 8 theorems describing liberation by random fracture, which had been extended to 19 theorems by the same author (Meloy et al., 1987) and extended a second time to overall 30 theorems by Barbery (1991). The main idea is, that the probability of cracks moving along grain boundaries is zero. Thus, no interfacial area is lost during comminution.

As pure random fracture and pure detachment are borderline cases, fracture mechanisms will be based on both to some extent. Therefore, King and Schneider (1998) described 6 different preferential breakage phenomena occurring in real grinding, which cover the field between random fracture and detachment. Previous studies proved preferential breakage to be occurring during grinding (Fandrich et al., 1997; King, 1994). It was found that the breakage is affected by mineral and particle properties. One example is the selective breakage of a softer component inside a multi-component material (Schranz and Berghöfer, 1958). Such hardness differences of various minerals within an ore can thus increase the amount of liberation by detachment during grinding (Hsih and Wen, 1994). Recently, mineral morphology was also related to fracture mechanisms (Singh et al., 2014). Mineral interfaces were classified into three classes (coherent, semi-coherent and incoherent) and their relation to the liberation characteristics has been discussed.

The speed of crack propagation and its role in transgranular and intergranular fracture has been discussed by Wills and Atkinson (1993). There the authors state, that small energy inputs and small strain rates will promote intergranular fracture. Using binary phase particles in slow compression tests, the effect of particle size on the strength of the particle was found to lead to enhanced grain boundary fracture (Bradt et al., 1995). Liberation by preferential grain boundary fracture was found to generally occur at a critical value of particle size (Bradt et al., 1995). Furthermore, preferential breakage has been measured on 3 mm cubic copper ore particles using X-ray microtomography (XMT) (Garcia et al., 2009). The authors proved the relation between preferential breakage along grain boundaries occurring in a compression test and the strain rate introduced to the material. When single particle breakage is studied, XMT may be the only way to investigate grain boundary fracture (Garcia et al., 2009).

XMT provides 3-dimensional data and gives thus the most complete picture of breakage along irregular shaped surfaces. It therefore was used in recent studies to investigate crack propagation (Charikinya and Bradshaw, 2014), particle damage (Kodali et al., 2011) as well

ACCEPTED MANUSCRIPT

as grain boundary fracture (Xu et al., 2013). XMT is based on grayscale images only and therefore lacks of a mineralogical characterization as different phases can have the same X-ray attenuation coefficient. New techniques like diffraction contrast tomography and correlative tomography (Maire and Withers, 2014) will help to enable mineralogical characterization for 3-dimensional features in the future. Besides the work done with XMT, Little and coworkers (2016) recently published an approach to quantify fracture along grain boundaries based on the conservation of the grain shape of chromite using auto SEM-EDS. They furthermore proved phase boundary fracture by comparing measured degrees of liberation as well as phase specific interfacial area with results of modelling under the assumption of random fracture.

In SEM-based automated mineralogy two-dimensional image analysis is used to measure three-dimensional sample features. This leads to a loss of one dimension during analysis which is known as the stereological bias. Nevertheless, there are material characteristics which can be measured without being biased. These characteristics are grades of components based on point (Thomson, 1930), line (Rosiwal, 1898) or area (Delesse, 1847) measurements and the surface area of components based on the length of boundaries (Barbery, 1991). A detailed description of the unbiased nature of grades and surface areas measured on slices of rock or grain mounts can be found in the book of Barbery (1991). It is important to understand, that these characteristics are valid for the particle population in total but will be biased when they are studied for an individual particle of the particle population.

Taking this into account there are restrictions when a change in surface area of minerals is studied to investigate grain boundary fracture. Samples for liberation measurement with a two-dimensional method have to be representative and in the case of grain mounts isotropic subsamples of the feed and the product of a comminution process. Thus segregation and preferential orientation of particles inside the mount must not be present. Results are valid for the material or mineral types in total. Therefore, the samples can neither be reduced to fractions of interest, nor is it valid to study individual particles or size classes of the product.

## 2. Theory

In particles of broken rock, the surface area (*SA*) of a mineral phase comprises of grain boundary areas between different mineral phases (interfacial area, *IA*) and free mineral surfaces (*FS*). The locked surface is the interfacial area of a mineral bound to other minerals. Free surface on the other hand is the mineral surface area which is not bound to other minerals.

$$SA = IA + FS \quad (1)$$

When two-dimensional methods are used, the liberation distribution is measured on a polished surface of an epoxy block. Thus volumes are represented by areas and areas are represented by lines (see Figure 1).

ACCEPTED MANUSCRIPT

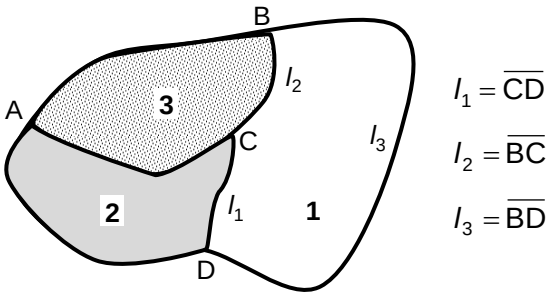


**Figure 1: Example showing a particle composed of 3 different grains. Points where 3 phases are in contact are named with A, B, C and D**

The surface of a mineral locked to other minerals is given by the length of the bordering lines of this phase to other phases. Referred to Figure 1 the interfacial area (*IA*) of phase 1 is given by $l_1 + l_2$. The free surface (*FS*) of phase 1 results in $l_3$.

Investigations on liberation and breakage phenomena are performed on particle populations. The surface areas are therefore represented by the sum of areas calculated on the individual particle sections. Different samples in liberation analysis will have different total numbers of particles visible in the sliced surface of an epoxy block. Thus absolute values of cumulative particle parameters like volume and surface have to be transferred to phase specific (*PS*) ones.

This is done by relating the particle surface to the particle volume. The phase specific surface area (*PSSA*) relates the mineral surface area to the mineral volume. In two-dimensional analysis this is given by the length of phase boundaries related to the area of this phase. In the same way interfacial areas and free surfaces can be transferred to phase specific parameters (phase specific interfacial area – *PSIA*, phase specific free surface - *PSFS*). Referring to Figure 1 this is given by equation (2).

$$PSSA = PSIA + PSFS = \frac{l_1 + l_2}{A_1} + \frac{l_3}{A_1} \qquad (2)$$

Using phase specific parameters furthermore enables comparing different minerals which typically differ in their proportions within a rock sample.

*PSSA* increases with decreasing particle size due to the generation of free surface through grinding. Having a phase locked inside another phase (inclusions), *PSSA* will remain constant until this phase starts to be liberated. New surface (*NS*) can only be generated by transgranular fracture. When detachment occurs, locked surface is liberated without the generation of new surfaces. That is why a change in *PSSA* is related to transgranular fracture mechanisms while grinding.

$$\Delta PSSA = NS \qquad (3)$$

If pure transgranular fracture takes place *PSIA* has to be constant with particle size. In other words, interfacial area is conserved in this case. This is one of the basic assumptions used in liberation modelling (Barbery, 1991; King, 1979; Meloy, 1984).

ACCEPTED MANUSCRIPT

The change in free surface area is a combination of new surface generated by transgranular fracture and the free surface generated by a loss of interfacial area between different minerals caused by intergranular fracture.

$$|\Delta PSFS| = |\Delta PSSA| + |\Delta PSIA| \quad (4)$$

When equation (4) is divided by the change in phase specific free surface, the amount of transgranular and intergranular fracture during breakage can be calculated.

$$1 = \left|\frac{\Delta PSSA}{\Delta PSFS}\right| + \left|\frac{\Delta PSIA}{\Delta PSFS}\right| \quad (5)$$

Given as a percentage equation (5) can be rewritten as

$$100\% = \text{x\% transgranular fracture} + \text{y\% grain boundary fracture} \quad (6)$$

Automated mineralogy on feed and product of comminution enables to measure changes of all three specific surface parameters. However, it needs to be emphasized that both samples have to represent the whole material. It is not valid just to analyze a specific size class. That is why selective breakage phenomena can lead to an enrichment of phases in different sizes.

When liberation characteristics of different minerals have to be compared based on minerals of different grain size distributions, a normalized size parameter is needed. Thus a normalized grain size (*ngs*), which is the mineral specific reduction ratio, is introduced.

$$ngs = \frac{x_{\text{m,product}}}{x_{\text{m,feed}}} \quad (7)$$

This normalized grain size relates the mean mineral grain size in the product particle population to the one in the feed. The mean mineral grain size $x_m$ is calculated based on equation (8) where $\Delta Q_3(x)$ is the fraction of the mineral grain size distribution found in an individual size class *i* and $\bar{x}_i$ is the mean size of this size class.

$$x_m = \sum \bar{x}_i \cdot \Delta Q_3(x) \quad (8)$$

For studies on an individual step of grinding, the mean mineral grain size in the feed of grinding has to be used. When fracture is studied over the whole chain of comminution the mineral grain size of the feed has to be the one in the original ore body.

The data needed for calculating $x_m$ using equation (8) can directly be taken from the mineral grain size distributions provided by MLA. In this study the size definition of an equivalent circle diameter (ECD) rather than equivalent ellipse (EE) or minimum bordering rectangle (MBR) was used for mineral grain size as well as particle size. Grain shape will not have an effect on the calculated parameters as these parameters are mineral specific. Hence, a difference in grain shape between different minerals e.g. elongated and isometric ones will not limit comparability of the results.

## 3. Materials and Method

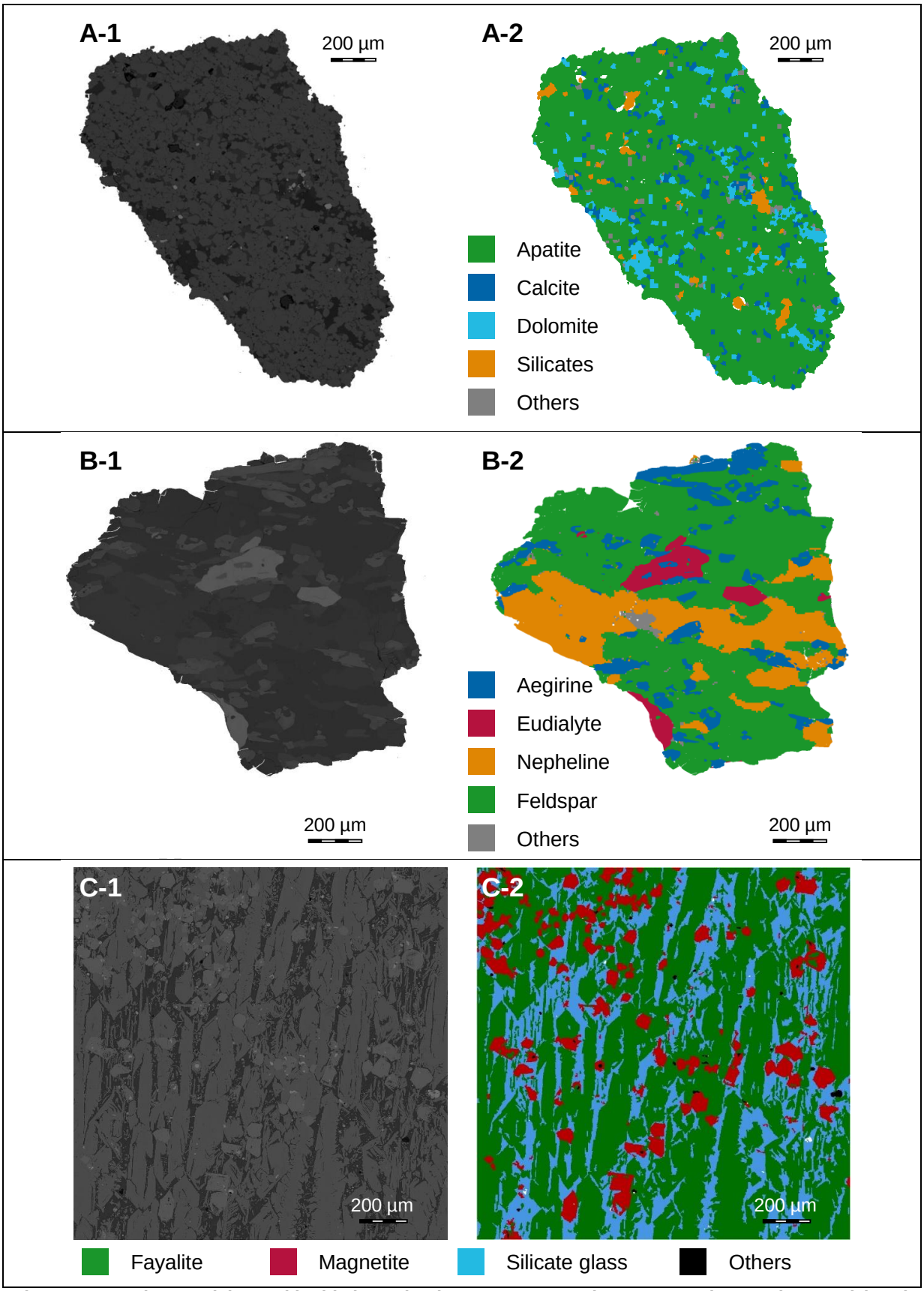


**Figure 2: Sample materials used in this investigation as representative BSE-SEM images (grayscale) and corresponding processed MLA images (false colored). A - apatite ore; B - nepheline-syenite; C - slag**

ACCEPTED MANUSCRIPT

## 3.1 Nepheline-Syenite

The nepheline-syenite sample originates from the Norra Kärr alkaline complex located in the south-eastern part of Sweden. The elliptical body covers an area of approximately 38,000 m² and is about 1,300 m long and in part 460 m wide. Nepheline-syenite is an igneous rock free of quartz (Le Bas and Streckeisen, 1991). The sample material mainly comprises of around 40 wt.-% feldspar, 22 wt.-% aegirine, 18 wt.-% zeolite, 9 wt.-% nepheline, 8 wt.-% eudialyte and 3 wt.-% others. The valuable component is the rare earth elements containing mineral eudialyte. The minerals inside the rock are locked in a relatively fine grained matrix, which requires grinding considerably below 0.2 mm for sufficient liberation (cf. Figure 2 B).

A sample of around 40 kg ore was comminuted in the facilities of UVR-FIA GmbH Freiberg. The rock was primarily broken to -3.15 mm using a laboratory jaw crusher followed by a ball mill. Grinding to product fineness was performed with subsamples of 5 kg in a screen discharge ball mill with screens of 2.0/1.0/0.5/0.25/0.125 mm. After grinding, the products were sieved into the size classes given in Table 1. Subsamples for MLA were taken from all size classes as well as from the un-sized grinding products.

**Table 1: List of the samples of the nepheline-syenite analyzed by MLA. The numbers given in the table represent the number of particle sections analyzed by MLA**

| | size classes in mm | | | | | | | |
|---|---|---|---|---|---|---|---|---|
| grinding | 2.0 - 4.0 | 1.0 - 2.0 | 0.5 - 1.0 | 0.25 - 0.5 | 0.125 - 0.25 | 0.063 - 0.25 | -0.063 | unsized |
| -2 mm | 338 | 788 | 1,697 | 4,550 | 14,275 | 41,079 | 203,769 | 13,290 |
| -1 mm | - | 937 | 1,341 | 4,012 | 11,886 | 35,539 | 204,688 | 100,176 |
| -0.5 mm | - | - | - | 8,157 | 14,912 | 41,182 | 204,657 | 142,812 |
| -0.25 mm | - | - | - | - | 12,931 | 46,043 | 203,784 | 151,192 |
| -0.125 mm | - | - | - | - | 16,180 | 36,462 | 203,191 | 165,995 |

## 3.2 Apatite ore

The apatite samples for this study were provided by the Vietnam Apatite Limited Company. It originates from a deposit in the Lao Cai province. With estimated reserves of about 820 million tons, it is one of the largest apatite-type ores in the Lao Cai province. The apatite ore primarily occurs in nature as marine sedimentary deposits. Sedimentary apatite ores can contain different forms of apatite (fluorapatite, chlorapatite and hydroxylapatite) based on the degree of ionic substitution within the lattice (Komar Kawatra and Carlson, 2014). The apatite ore investigated in this study comprises of sedimentary carbonaceous fluorapatite (68 wt.-%) and gangue minerals like dolomite (19 wt.-%), calcite (5 wt.-%), silicates (5 wt.-%), ankerite (1 wt.-%) and 2 wt.-% others. The gangue minerals are finely disseminated inside a matrix like structure of coarse grained apatite (cf. Figure 2 A).

The entire sample of about 150 kg was crushed at the Institute of Mechanical Process Engineering and Mineral Processing, TU Bergakademie Freiberg. The crushing was done in three steps jaw crusher – cone crusher – roller mill with gap widths of 50 mm, 15 mm and 2 mm, respectively. The apatite ore sample below 2 mm particle size was then split by sample rifflers and used as feed for milling tests. The batch milling tests were done on subsamples of 2 kg in a laboratory ball mill. The grinding time was varied in the steps 4, 6, 8 and 10 minutes. Subsamples of feed as well as grinding products were taken by spinning sample rifflers and handed to liberation analysis. A single particle mount was produced of each subsample without preliminary preparation of size classes. The particle sections analyzed per mount are listed in Table 2.

ACCEPTED MANUSCRIPT

**Table 2: List of the samples of the apatite ore analyzed by MLA (feed and products from milling). The numbers given in the table represent the number of particle sections analyzed by MLA.**

| Sample | feed | 4 min | 6 min | 8 min | 10 min |
|---|---|---|---|---|---|
| No. of particles | 15,682 | 77,163 | 70,875 | 70,410 | 26,410 |

## 3.3 Slags

The investigated slag is a waste material from a smelter of a copper porphyry mine. It mainly comprises of silicate and oxide mineral phases. So far, the slag is stockpiled in a dump which leads to major environmental problems for the mine and the surrounding area. The main slag phase is fayalite, accounting for around 60 wt.-%. This high temperature, iron rich olivine forms elongated dendritically crystals which dominate the sample structure (cf. Figure 2 C). In between and to a large extend associated with fayalite is an aluminum silicate glass, matrix like phase. This silicate accounts for about 18 wt.-% of the sample. Ten weight percent of the sample consists of magnetite showing a typical spinifex texture.

The slag sample first was crushed with a jaw crusher followed by a roller mill to a defined upper particle sizes of 1.5 mm and then ground to product fineness using a planetary ball mill. The milling was done at three different grinding times of 6, 7 and 10 minutes. After grinding, the material was sieved into the size classes given in Table 3. All size classes of the feed and the grinding products were passed on to mineral liberation analysis. Based on the mass balance the results of analysis were back calculated to the total samples.

**Table 3: List of the samples of the slags analyzed by MLA (feed and products from milling). The numbers given in the table represent the number of particle sections analyzed by MLA.**

| | size classes in µm | | | |
|---|---|---|---|---|
| grinding | -40 | 40 - 56 | 56 - 71 | +71 |
| feed | 198,013 | 172,660 | 130,449 | 16,304 |
| 6 min | 231,992 | 171,883 | 97,742 | 26,969x |
| 7 min | 229,603 | 155,179 | 91,170 | 59,022 |
| 10 min | 210,144 | 22,353 | - | - |

## 3.4 Mineral liberation analysis

The feed materials as well as the products of the milling tests on the three materials were handed to automated mineralogy (Mineral Liberation Analyzer, MLA). In order to analyze the loose material from milling it was mounted in an epoxy block. Therefore aliquots of 3 g of solid material were mixed with graphite and epoxy resin. Resulting sample blocks (30 mm in diameter) were ground and polished at the Sample Preparation Lab of the Helmholtz Institute Freiberg for Resource Technology. Before using the SEM, the polished epoxy blocks are carbon coated with a Leica (Baltec) MED 020 vacuum evaporator to ensure conductivity of the sample surface.

The MLA comprises a FEI Quanta 650F SEM (FE-SEM) equipped with two Bruker Quantax X-Flash 5030 EDX detectors and FEI's MLA suite 3.1.4 for data acquisition. Identification of mineral grains by MLA is based on backscattered electron (BSE) image segmentation and collection of EDX-spectra of the particles and grains distinguished in BSE-imaging mode. Collected EDX-spectra are then classified using a list of standard mineral spectra collected by the user. More detailed information on the functionality of the MLA system can be found in *Fandrich* et al. (2007) and *Gu* (2003). A description of the exact analytical procedure is provided by *Sandmann and Gutzmer* (2013). The MLA measurements were carried out at

ACCEPTED MANUSCRIPT

the Geometallurgy Laboratory at TU Bergakademie Freiberg and the Helmholtz Institute Freiberg.

In this study, the GXMAP measurement mode was applied on all samples. Consistent operating conditions were applied using 10.0 nA probe current at 25 kV and a working distance of 12 mm. Calibration of contrast and brightness was set as such that the epoxy resin showed a BSE grey level of 8 and gold a BSE grey level of 254. Depending on the material, the resolution and therefore the pixel size varied between 0.8 and 3.4 µm/pixel. A step size of 6x6 pixel and a minimum EDX count of 2000 were applied. The minimum particle and minimum grain size were set to 4 pixels. Dependent on the particle size, between 300 to more than 200,000 particle sections were analyzed on each single polished sample surface (c.f. Tables 1, 2 and 3).

The evaluation of the MLA measurements provides information on the qualitative and quantitative mineralogy as well as the grain size distribution and mineral liberation. In this study, grain size distribution and liberation are the main attributes assessed. Data processed with the Mineral Liberation Analyzer does not comprise stereological transformation (Fandrich et al., 2007). If there is written about liberation in this study, it is always related to two-dimensional data.

## 3.5 Calculations

This section gives a briefly description of the calculations done for this study and the output information from MLA on which the calculations are based on. Besides what was written in the theory section, some special calculations were done for data adjustment before analysis.

In the first step, the data from size classes must be combined by their mass fractions from sieving to cover the entire sample. This was done for the nepheline-syenite and the slag sample using the combine function in MLA-view software. In case of the apatite ore un-sized material was analyzed by MLA. To adjust the data of the apatite ore, its particle size distribution from analytical sieving was used. Therefore the particle population from MLA-data of the un-sized sample was virtually sieved into the size fractions from analytical sieving using filters for ECD. These virtual size classes were than recombined using the mass fractions from analytical sieving.

In the second step, the tables “Modal Mineralogy”, “Phase Specific Surface Area” and “Mineral Association” as well as the particle size distribution and the mineral grain size distributions were exported from MLA-view software to Microsoft Excel. When the combine function in MLA-view is applied to the data, information on “Mineral Boundary” and “Mineral Area” is lost, as it is not valid to combine these parameters. This is due to the fact, that the mineral area as well as the mineral boundary visible in a section of a mount is a function of the random particle concentration in the epoxy. Therefore “Area-%” of the minerals from “Modal Mineralogy” table together with *PSSA* and a user defined “Total Area” (can be any value as it is of random nature) must be used to calculate the missing parameters. Having the “Mineral Boundary” (equals the perimeter given in µm) and the “Mineral Area” (total area of mineral sections given in µm²) the *PSFS* and *PSIA* can be calculated using the information of the “Mineral Association” table. The mean mineral grain sizes were calculated using equation 8 and the data from “Mineral Grain Size Distribution” table (size definition: equivalent circle diameter, ECD).

ACCEPTED MANUSCRIPT

In the last step, the parameters *PSSA*, *PSIA*, *PSFS* of the feed and the grinding products were compiled to calculate the change in these parameters (see equation 4). Then the percentage of detachment (grain boundary fracture) and the percentage of transgranular fracture are calculated based on equation 5. The *ngs* is calculated by equation 7 using the mean mineral grain sizes of the grinding products and from the feed to grinding. Depending on the scope of investigation, the *ngs* can also be related to the original grain size distribution in the ore body. All results discussed in the following sections are related to the mineral grain size distribution in the grinding feed.

# 4. Results

## 4.1 Nepheline-Syenite

When measurements are done on mounts of sample material having a wide size distribution, fines get underestimated and measured particle size distributions will be biased. In case of isotropic mounts there should be no such effect, thus basics of stereology are valid (Barbery, 1991) and size distributions from image analysis fit to sieving data when the material has a wide size distribution (Petruk, 1978). Having material of a wide size distribution in a mount the risk of segregation arises and isotropy can be lost. Figure 3 shows the particle size distributions from MLA of the sieved and the un-sieved sample besides the cumulative mass fraction from analytical sieving of the sample -2000 µm. It can clearly be taken from the figure, that there is a large difference between the size distribution from un-sieved material and the sieving data. Fines are strongly underestimated in the size distribution coming from MLA. Following Petruk (1978) this should not be the case and can be addressed to segregation.

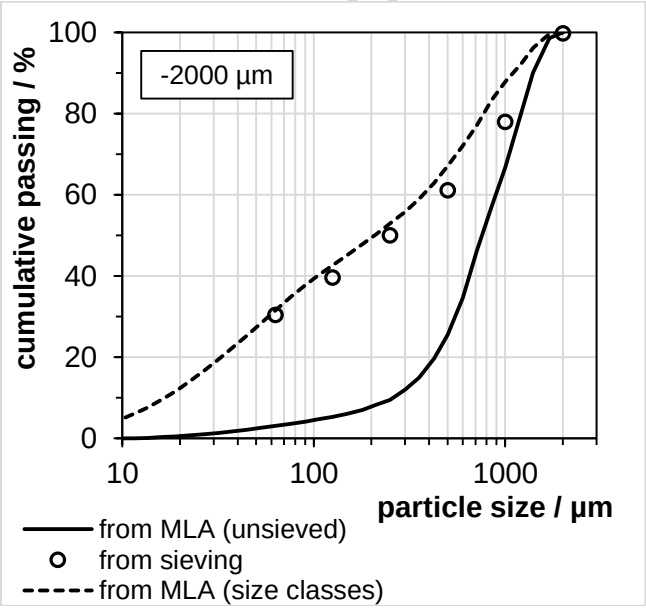


**Figure 3: Comparison of particle size distributions from MLA for the unsieved sample as well as for the sized material of the nepheline-syenite (size definition ECD). The distribution from analytical sieving is shown by the rings.**

To prevent errors caused by segregation, grain mounts were produced from size classed material as described in the above sections. After combining the data of the size classes to a virtual total sample using the mass fractions, the particle size distributions from MLA fit to the cumulative mass fractions from sieving. This is shown in Figure 4 for all samples of the nepheline-syenite.

ACCEPTED MANUSCRIPT

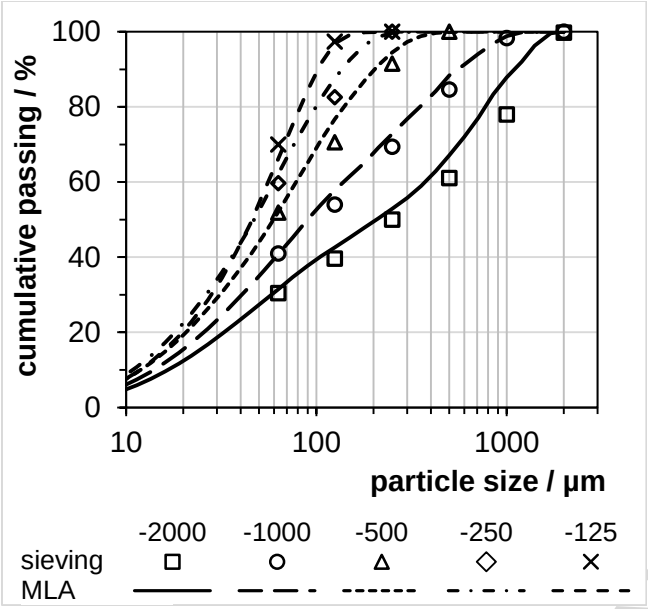


**Figure 4: Comparison of sieving data and particle size distributions from MLA (size definition ECD) for the five different mill products of the nepheline-syenite.**

Table 4 exemplarily lists the data for un-sieved and sieved material given for the coarsest grinding product of the nepheline-syenite. Nearly all parameters differ in the data of the samples prepared by the two procedures. As long as there is no de-mixing due to different specific gravity of minerals or enrichment of minerals in specific sizes, the mineral grades should be equal in results from sieved and un-sieved material. The slightly different grades given in Table 4 cannot with certainty be used as an indicator for de-mixing occurring in the un-sieved sample. Such small differences can also arise from small measurement errors and the mathematical combination using the mass fractions.

Distinct to the mineral grades all the other parameters listed in Table 4 are affected by the underestimation of fines. Fines are characterized by their higher specific surface and better liberation. Thus all parameters of the particle population, which are related to its surface, will differ when the amount of fines in a sample changes. An increased amount of fines also affects the particle size distribution and the mineral grain size distribution. The difference in the latter one will be small as long as the mineral grain sizes are small compared to the particle sizes (c.f. Aegirine).

**Table 4: Compilation of different parameters from MLA of the un-sieved and the size classed sample from the -2.0 mm material**

| Mineral | grade wt.-% | PSSA µm$^{-1}$ | FS % | PSIA µm$^{-1}$ | PSFS µm$^{-1}$ | grain size µm |
|---|---|---|---|---|---|---|
| data from un-sieved sample | | | | | | |
| Aegirine | 13.6 | 0.136 | 13.11 | 0.118 | 0.018 | 79.4 |
| Eudialyte | 6.8 | 0.077 | 22.59 | 0.060 | 0.017 | 167.7 |
| Nepheline | 12.7 | 0.059 | 20.49 | 0.047 | 0.012 | 308.7 |
| Feldspar | 40.6 | 0.057 | 28.08 | 0.041 | 0.016 | 383.2 |
| Zeolite | 18.2 | 0.059 | 25.14 | 0.045 | 0.015 | 341.2 |
| data from size classed samples | | | | | | |
| Aegirine | 14.7 | 0.196 | 46.65 | 0.104 | 0.091 | 59.5 |
| Eudialyte | 8.0 | 0.185 | 53.53 | 0.086 | 0.099 | 105.6 |
| Nepheline | 10.5 | 0.130 | 40.06 | 0.078 | 0.052 | 175.8 |
| Feldspar | 40.1 | 0.147 | 53.80 | 0.068 | 0.079 | 186.4 |

ACCEPTED MANUSCRIPT

| | | | | | | |
|---|---|---|---|---|---|---|
| Zeolite | 18.3 | 0.136 | 49.30 | 0.069 | 0.067 | 196.2 |

The diagrams of Figure 5 show the main results of the grinding experiments of the nepheline-syenite. In the feed sample the five main mineral groups differ in mineral grain size distribution. A fine grained aegirine is found besides coarser grained eudialyte, nepheline, zeolite and feldspar (cf. Figure 5, A). Related to the mineral grain size, aegirine shows high values in *PSSA* and *PSIA* in the feed sample. Interestingly the parameters of eudialyte are in the same range as the ones of aegirine even though its grain size distribution is coarser than the one of aegirine. Thus surface roughness of eudialyte is higher compared to aegirine.

As expected, *PSFS* increases with the fineness of grind. Thus minerals get liberated. The *PSIA* decreases with decreasing particle size. This indicates that grain boundary area is lost and detachment takes place. The decrease of *PSIA* is in the same range for all mineral groups under investigation.

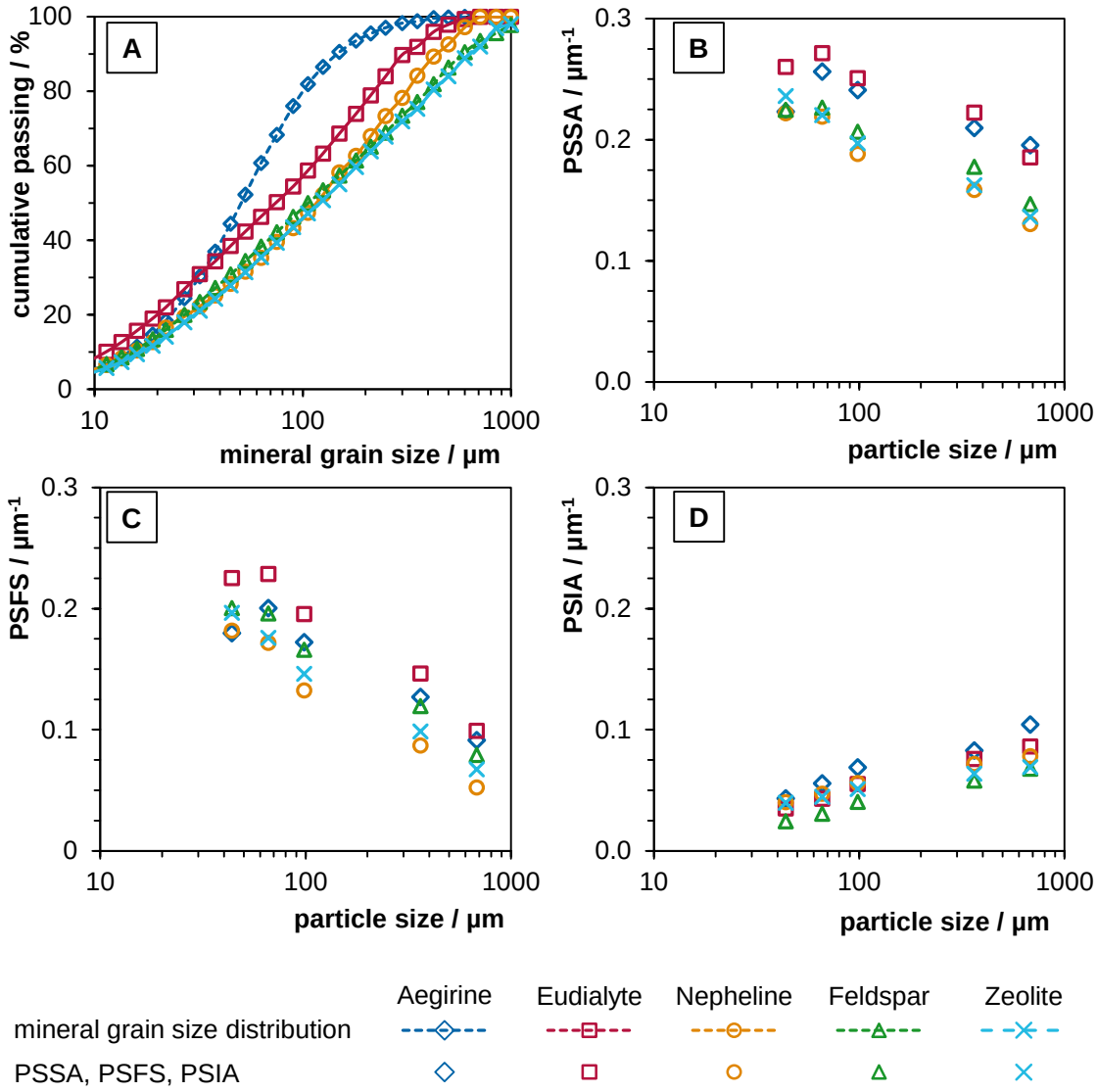


**Figure 5: Compilation of parameters for the main mineral phases in the nepheline-syenite. A: cumulative mineral grain size distribution in the -2.0 mm material (size definition ECD), B: phase specific surface area (PSSA), C: phase specific free surface (PSFS) and D: phase specific interfacial area (PSIA). Particle size in B, C and D given as geometric mean size using equation 8.**

ACCEPTED MANUSCRIPT

By using the approach presented in chapter section 2 the extent of detachment (which is intergranular fracture) on surface exposure can be calculated. When this parameter is plotted against the *ngs* of the minerals their fracture characteristic becomes comparable (cf. Figure 6). It can be seen, that there is a significant difference in the liberation characteristic of aegirine and the other minerals. Aegirine shows a higher percentage of detachment on the generation of free surface. This can be addressed to the liberation characteristic of aegirine but is also affected by less transgranular fracture leading to larger *ngs*. The other four mineral groups tend to mainly liberate by transgranular fracture.

An interesting trend can be seen for eudialyte, nepheline and feldspar, which show an increasing percentage of detachment with decreasing *ngs*. An effect like this is already described in the literature (Bradt et al., 1995) and can be addressed to a change in the relation of the strengths of grain boundaries and the locked phases. The smaller the particles become, the fewer inclusions and inhomogeneities are inside the phases where cracks can be initiated.

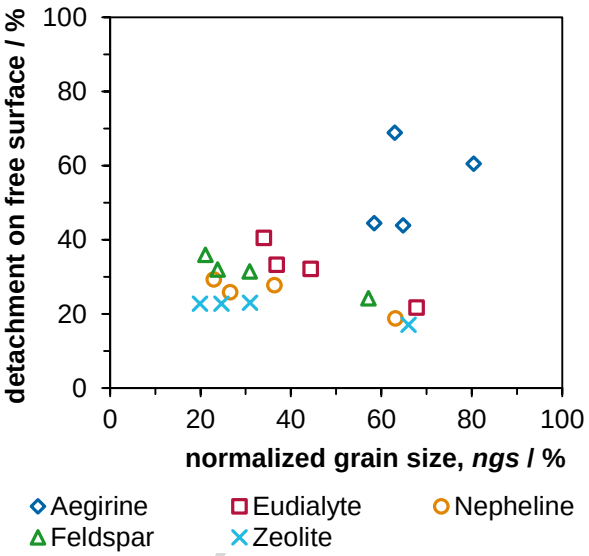


**Figure 6: Percentage of detachment (preferential breakage) on the generation of free surface for the nepheline-syenite ore**

It has to be mentioned, that the data of aegirine seems to scatter. The data point of aegirine in Figure 6 showing the largest percentage of detachment belongs to the finest grinding product but does not have the smallest *ngs*. This is believed to be caused by a statistical bias and the small differences in mean mineral grain sizes which are transferred into a relative number given as *ngs*.

## 4.2 Apatite ore

As there were no size classes analyzed by MLA for the apatite ore samples, the data was checked on consistency based on the size distribution from MLA and the cumulative mass fraction from analytical sieving. It was found that fines are strongly underestimated in the MLA data compared to analytical sieving. Figure 7 shows both distributions together with a size distribution of a virtually sized and recombined sample. The latter one was created by virtual sieving using size filters defined in MLA-view software followed by a recombination of

ACCEPTED MANUSCRIPT

these size classes using the mass fractions known form analytical sieving (c.f. Table 5). The data adjusted by this alternative approach was used for the investigation done in this study.

**Table 5: Mass fraction of size classes from analytical sieving and of size classes from virtual sieving of the MLA sample using filters in MLA-view software (size definition ECD)**

| size class | MLA | sieving |
|---|---|---|
| µm | wt.-% | wt.-% |
| +500 | 75.0 | 42.0 |
| 200…500 | 15.5 | 17.3 |
| 71…200 | 3.6 | 9.7 |
| -71 | 5.9 | 31.0 |

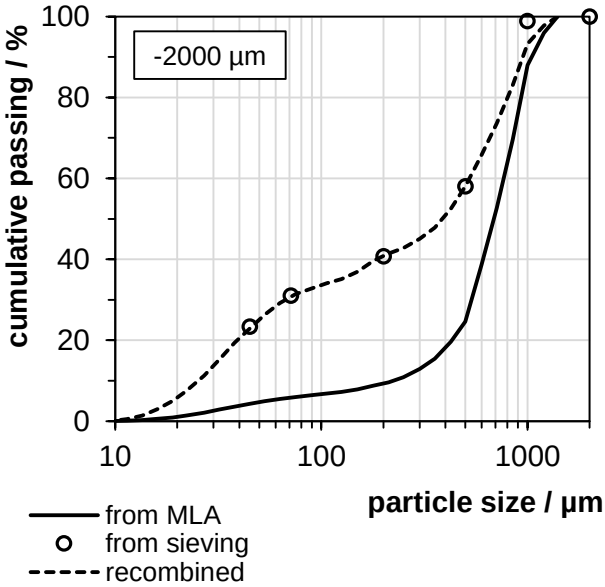


**Figure 7: Comparison of particle size distributions from MLA for the unsieved sample as well as for the sized material of the apatite ore (size definition ECD). The distribution from analytical sieving is shown by the rings.**

Comparing the data of the un-sieved sample with the virtually sieved and recombined one given in Table 6, the consistency in the mineral grades is very good. Thus, there is no change in composition caused by data adjustment. The change in the surface related parameters as well as in grain size equals what was found above for the nepheline-syenite system. An increased amount of fines increases the free surface, the *PSSA* and *PSFS* while *PSIA* and mean mineral grain sizes are reduced. It is therefore believed, that the approach of using electronical sieving followed by a recombination of these virtual size classes based on the mass fractions from analytical sieving gives similar results to the use of size classes in MLA.

**Table 6: Compilation of different parameters from MLA of the original un-sieved sample and the reconstructed sample from electronic sieving**

| | **grade** | **PSSA** | **FS** | **PSIA** | **PSFS** | **grain size** |
|---|---|---|---|---|---|---|
| **Mineral** | **wt.-%** | **µm$^{-1}$** | **%** | **µm$^{-1}$** | **µm$^{-1}$** | **µm** |
| original data from un-sieved sample | | | | | | |
| Apatite | 68.1 | 0.066 | 32.64 | 0.044 | 0.022 | 511.0 |
| Ankerite | 1.0 | 0.303 | 5.67 | 0.286 | 0.017 | 20.5 |
| Calcite | 4.9 | 0.181 | 10.53 | 0.162 | 0.019 | 105.8 |

ACCEPTED MANUSCRIPT

| | | | | | | |
|---|---|---|---|---|---|---|
| Dolomite | 19.0 | 0.123 | 14.58 | 0.105 | 0.018 | 192.1 |
| Silicates | 4.8 | 0.137 | 17.97 | 0.112 | 0.025 | 110.1 |
| Others | 3.2 | 0.193 | 12.26 | 0.169 | 0.024 | - |
| electronic sieving and recombination using mass fraction from analytical sieving | | | | | | |
| Apatite | 68.8 | 0.102 | 47.29 | 0.054 | 0.048 | 321.5 |
| Ankerite | 0.9 | 0.301 | 16.04 | 0.253 | 0.048 | 20.4 |
| Calcite | 4.5 | 0.188 | 27.65 | 0.136 | 0.052 | 81.5 |
| Dolomite | 18.4 | 0.139 | 31.53 | 0.095 | 0.044 | 140.0 |
| Silicates | 5.5 | 0.150 | 44.00 | 0.084 | 0.066 | 82.7 |
| Others | 2.0 | 0.233 | 25.18 | 0.175 | 0.059 | - |

As can be seen in the mineral grain size distributions (cf. Figure 8 A), the apatite ore comprises of coarse grained apatite and finer grained dolomite, calcite and silicates. To achieve sufficient liberation of small grained minerals, the coarse apatite has to be broken down to the size of the interlocked minerals. Thus transgranular fracture of apatite is needed.

Comparing specific mineral surface parameters, the effect of size is obvious. Calcite shows the highest values in *PSSA* (cf. Figure 8 B) and *PSIA* (cf. Figure 8 D) of the feed (points on the coarse end of the diagrams) as it is the finest grained mineral. The coarse grained apatite (on the other hand) shows small values in *PSSA* and *PSIA* in the feed. *PSFS* (cf. Figure 8 C) of all minerals in feed is small as no significant surface exposure occurs in the previous crushing steps.

During comminution, the particle size is reduced and new free surface is generated (cf. Figure 8 C) either by transgranular or by intergranular fracture. Figure 8 D clearly indicates that there is a loss in *PSIA* which only can be due to intergranular fracture. When free surface is generated by transgranular fracture, *PSSA* (cf. Figure 8 B) increases. With respect to apatite the increase in *PSSA* for dolomite, calcite and silicates is small. Therefore these minerals are mainly liberated by intergranular fracture (detachment).

ACCEPTED MANUSCRIPT

ACCEPTED MANUSCRIPT

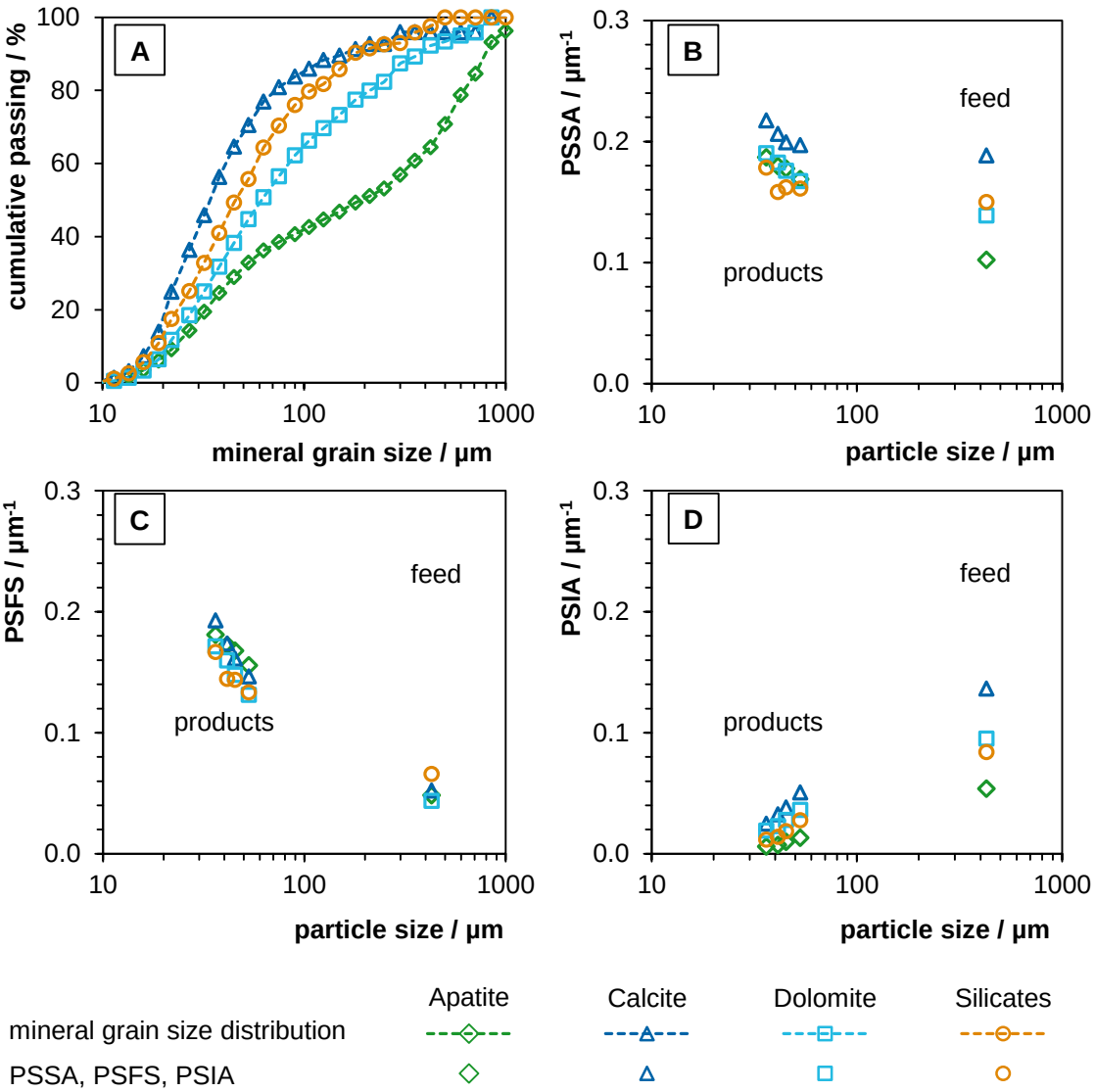


**Figure 8: Compilation of parameters for the main mineral phases in the apatite ore. A: cumulative mineral grain size distribution in the feed (size definition ECD), B: phase specific surface area (PSSA), C: phase specific free surface (PSFS) and D: phase specific interfacial area (PSIA). Particle size in B, C and D given as geometric mean size using equation 8.**

When the percentage of detachment is plotted against the *ngs*, the different liberation characteristic of the mineral groups can be visualized (cf. Figure 9). With decreasing normalized grain size the percentage of detachment on the generation of free surface decreases for all mineral groups of the ore. This is due to the generation of new surface by comminution of coarse grains.

The coarse grain size distribution of apatite combined with grinding to a specific fineness results in small normalized grain sizes. Furthermore, high reduction ratios of apatite lead to a generation of free surface by transgranular fracture. Thus the percentage of detachment on generated free surface is small.

Dolomite, calcite and silicates show values of more than 50 % detachment. These minerals tend to be liberated by intergranular fracture. A difference in the liberation characteristic of the carbonates can be related to the difference in *ngs*. The size of the coarser grained dolomite has been reduced by transgranular fracture, which consequently leads to a decrease in the percentage of detachment.

ACCEPTED MANUSCRIPT

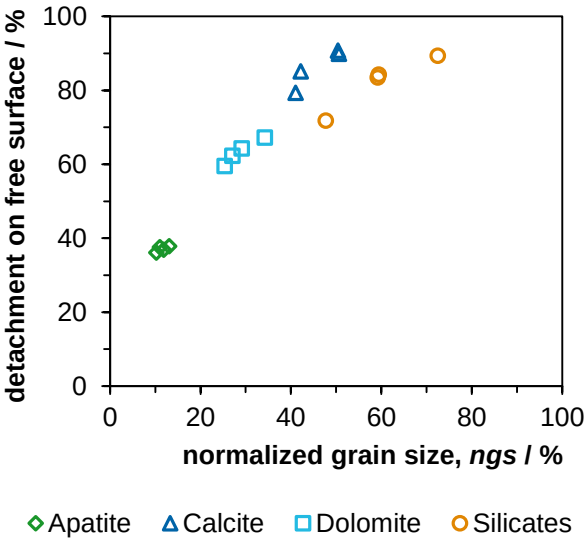


**Figure 9: Percentage of detachment (intergranular fracture) on the generation of free surface for the apatite ore**

## 4.3 Slags

The parameters of the slags investigated in this study differ strongly from the ones of the two ores discussed above. This artificial material comprises of very fine grained phases (cf. Figure 10 A) which are bonded together by rough surfaces (see materials paragraph and the points representing the feed in Figure 10 B). Due to the structure of mineral boundaries and the brittle breakage behavior, it will be difficult to liberate by intergranular fracture (shown in Figure 10 B – D). *PSSA* and *PSFS* strongly increase with decreasing particle size.

Distinct to the other specific surface parameters the *PSIA* nearly remains constant until a defined fineness is reached. From this point intergranular fracture leads to a loss of interfacial area (Figure 10 D). At larger *ngs* only silicate phases seem to be exposed by a small amount of intergranular fracture from the beginning of the grinding. Overall the loss of interfacial area with the fineness of grind is small. Therefore the slags can be addressed to material which mainly are liberated by random fracture.

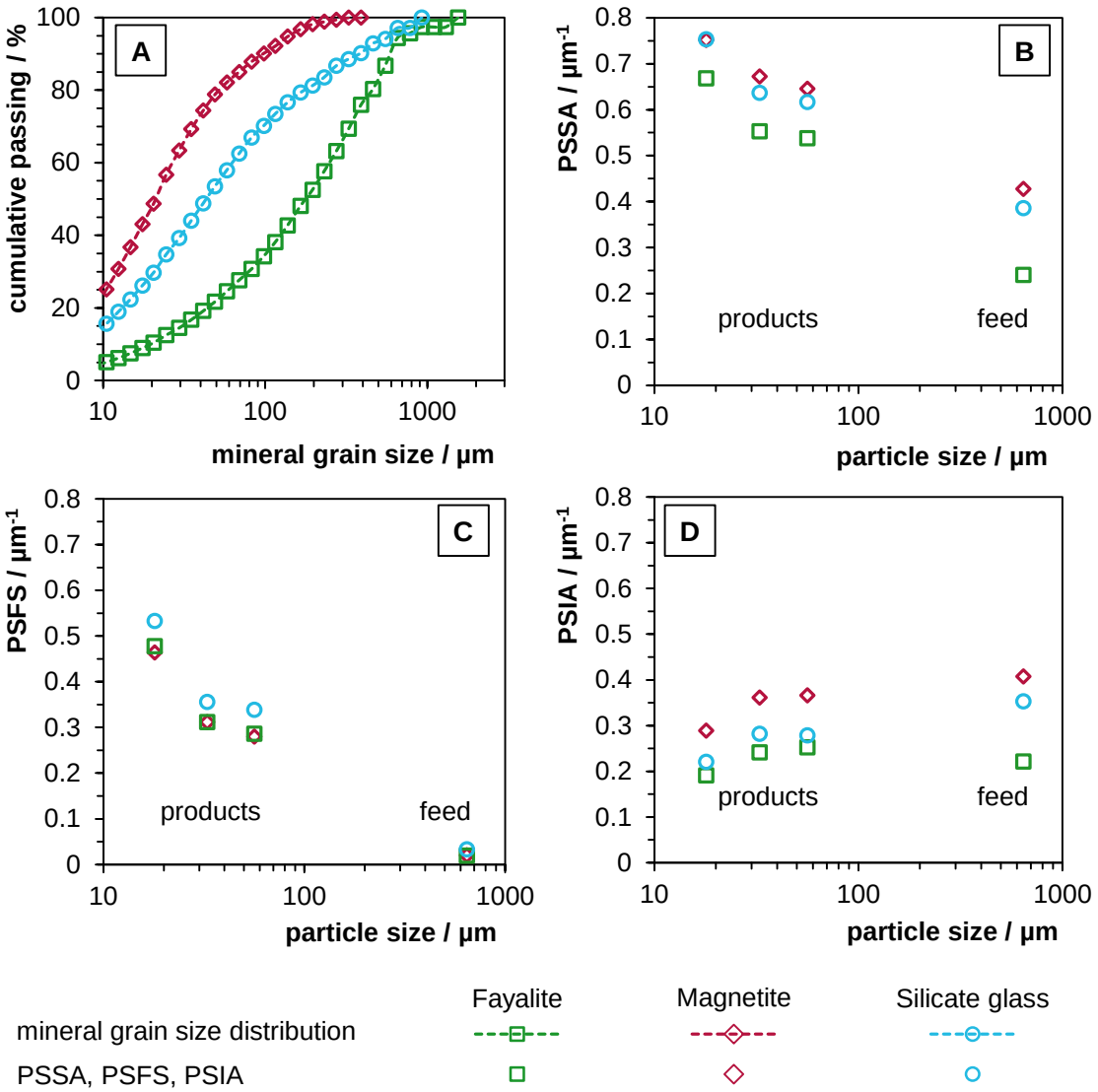


**Figure 10: Compilation of parameters for the main mineral phases in the copper slags. A: cumulative mineral grain size distribution in the feed (size definition ECD), B: phase specific surface area (PSSA), C: phase specific free surface (PSFS) and D: phase specific interfacial area (PSIA). Particle size in B, C and D given as geometric mean size using equation 8.**

It has to be mentioned, that there is an inconsistency in the data of the slags. The parameter *PSIA* is slightly increasing from feed of grinding to the grinding products of 6 and 7 minutes grinding time. Theoretically, this is not possible and can only be addressed to reduced comparability of the sample data coming from MLA. Having a close look on the raw data, the fayalite grade of the feed is smaller compared to the grinding product by around 5 wt.-%. The grade of silicates is larger by around the same amount. Grades of other minerals are not affected.

Similar to the nepheline-syenite, some mineral groups in the slags show an increasing percentage of detachment when mineral grain size is reduced (cf. Figure 11). Such an increasing amount of detachment can be studied for magnetite and silicates. This is related to the generation of minerals in the slags during cooling. The crystallization order is magnetite - fayalite - silicate glass. Therefore magnetite mainly is surrounded by silicate phases. When magnetite gets detached from its silicate glass partner, the amount of detachment for both minerals increases.

ACCEPTED MANUSCRIPT

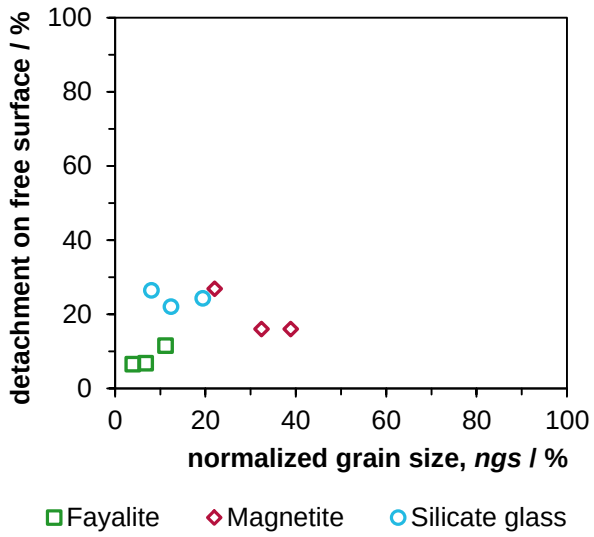


**Figure 11: Percentage of detachment (preferential breakage) on the generation of free surface for the copper slags**

## 5. Discussion

There are significant differences in the liberation characteristic of different materials. The minerals in the apatite ore, which is a sedimentary rock, show high proportions of detachment on the generation of free surface even at high reduction ratios. In contrast, minerals in the nepheline-syenite seem to mainly be liberated by random fracture. In slags, which are artificial materials, the percentage of detachment is very low. This can be explained by their anisotropic structure and their rough interfaces compared to the natural rocks. The liberation characteristic not just differs between different materials it also differs between minerals within a specific material. This can be seen for the minerals in the nepheline-syenite ore.

Eudialyte, nepheline and feldspar in the nepheline-syenite as well as silicates and magnetite in the slags were found to have an increasing percentage of detachment at high reduction ratios. This is in good agreement with the model published by *Bradt* (1995). This model states, that the strength of phase boundaries is stronger than one of the phases locked together. During comminution the amount of defects and cracks inside a phase decreases. This leads to an increasing strength of phases until their strength is higher than the ones of phase boundaries. From this point on detachment takes place (Bradt et al., 1995).

Detachment can also occur right from the beginning of comminution, as long as the strength of phase boundaries is weaker than the one of the locked phases. This can be seen in the liberation characteristic of the apatite ore. It may be true for some types of sedimentary rock in general. On the other hand, phases which are locked together by rough grain boundaries will be difficult to liberate by detachment (e.g. slags). When there is a dendritic texture, phases will mainly be liberated by transgranular fracture.

Some minerals showed a size dependent amount of detachment on mineral surface exposure. Therefore, the definition of a single detachment factor to model mineral liberation (Hsih and Wen, 1994) needs to be developed carefully and may be extended to detachment functions. Selective fracture mechanisms which were discussed by different authors in the

ACCEPTED MANUSCRIPT

past (Fandrich et al., 1997; King, 1994) have not been investigated in this work and will be part of future studies.

Mineral properties, like hardness, cleavage and crystal structure are reported to have an influence on the amount of detachment on surface exposure (Hsih and Wen, 1994; Singh et al., 2014). It is a difficult task to define these properties on materials with complex mineralogy, for mineral groups like zeolite or for phases like aluminum silicate glass in the slag. Therefore, no such relation was found for the materials under investigation.

Ball milling, which was used to grind the different materials, is known to be an unselective type of grinding (Veasey and Wills, 1991). That is why the milling cannot be the source for enhanced selective breakage or improved grain boundary fracture. Thus effects found in this study can be addressed to be material characteristic. This finding is in good agreement with results recently published by Little and coworkers (2016) for a platinum group element ore from South Africa, which showed significant amounts of grain boundary fracture in ball milling. There is a large variety of parameters, like structure, mechanical properties, morphology and roughness of boundary areas, grain size, cracks and flaws of minerals in rocks or phases in artificial materials influencing the fracture. Fundamental work on the role of these parameters on the fracture of materials can help to understand and influence liberation by intergranular fracture.

## 6. Conclusions

Two-dimensional SEM-based automated mineralogy can be used to investigate the extent of transgranular and intergranular fracture on surface exposure when the following constraints are fulfilled:

- The samples have to cover the entire material (feed or product) of a comminution process.
- All samples have to be measured using the same resolution and horizontal field width. Otherwise the fractal effect has to be considered.
- When samples were fractioned before analysis, a back calculation based on the mass balance is necessary. It has to be considered, that only specific parameters can be used in back calculation as lengths of boundaries and mineral areas depend on the amount of particles visible in the sliced surface of the epoxy block. This amount of visible particles is random and does not have any relation to the mass balance.
- Parameters for surface area, free surface and interfacial area have to be calculated as mass or volume specific ones.
- Results are valid for the overall material. It is not possible to draw conclusion for single particles within the samples.

This case study on different materials shows material specific breakage behavior. Furthermore a size specific change in the extent of transgranular and intergranular fracture on surface exposure was found. This is in good consistency with literature.

Different minerals or phases inside a material differ in breakage and liberation characteristics. Further studies on the role of material properties, morphology of boundary area and cracks have to be performed to understand and influence intergranular fracture for

ACCEPTED MANUSCRIPT

improved liberation. This will help to liberate at coarser grind which directly leads to energy savings.

## Acknowledgements

Research for this study was mainly performed at the research groups of Mineral Processing at the Institute of Mechanical Process Engineering and Mineral Processing, TU Bergakademie Freiberg and Helmholtz-Zentrum Dresden-Rossendorf, Helmholtz Institute Freiberg for Resource Technology. It was supported and benefited from numerous discussions and measurements by Petya Atanasova, Andreas Bartzsch and Sabine Haser.

The authors would like to acknowledge Vietnam Apatite Limited Company and colleagues from the Department of Mineral Processing, Hanoi University of Mining and Geology for apatite ore sample provision and preparation to transport to Germany. Furthermore, the authors are particularly indebted to Tasman Metals Ltd. for providing rock samples and useful information about the Norra Kärr deposit.

## References

Barbery, G., 1991. Mineral Liberation Measurement, Simulation and Practical Use in Mineral Processing, Québec, Canada.
Barbery, G., 1992. Liberation 1, 2, 3: Theoretical analysis of the effect of space dimension on mineral liberation by size reduction. Minerals Engineering 5, 123–141.
Bradt, R.C., Lin, C.L., Miller, J.D., Chi, G., 1995. Interfacial fracture of multiphase particles and its influence on liberation phenomena. Minerals Engineering 8, 359-366.
Charikinya, E., Bradshaw, S., 2014. Use of X-ray computed tomography to investigate microwave induced cracs in sphalerite ore particles, XXVII International Mineral Processing Congress IMPC 2014, Santiago (Chile).
Delesse, M.A., 1847. Procédé méchanique pour déterminer la composition des roches. Comptes Rendus de l'Académie des Sciences 25, 544-548.
Fandrich, R., Gu, Y., Burrows, D., Moeller, K., 2007. Modern SEM-based mineral liberation analysis. International Journal of Mineral Processing 84, 310-320.
Fandrich, R.G., Bearman, R.A., Boland, J., Lim, W., 1997. Mineral liberation by particle bed breakage. Minerals Engineering 10, 175-187.
Garcia, D., Lin, C.L., Miller, J.D., 2009. Quantitative analysis of grain boundary fracture in the breakage of single multiphase particles using X-ray microtomography procedures. Minerals Engineering 22, 236-243.
Gaudin, A.M., 1939. Principles of Mineral Dressing. McGraw-Hill, New York.
Gu, Y., 2003. Automated Scanning Electron Microscope Based Mineral Liberation Analysis: An Introduction to JKMRC/FEI Mineral Liberation Analyser. Journal of Minerals & Minerals Characterization & Engineering 2, 33–41.
Hsih, C.S., Wen, S.B., 1994. An extension of Gaudin's liberation model for quantitatively representing the effect of detachment in liberation. International Journal of Mineral Processing 42, 15-35.
King, R.P., 1979. A model for the quantitative estimation of mineral liberation by grinding. International Journal of Mineral Processing 6, 207-220.
King, R.P., 1994. Linear stochastic models for mineral liberation. Powder Technology 81, 217-234.

ACCEPTED MANUSCRIPT

King, R.P., Schneider, C.L., 1998. Mineral liberation and the batch comminution equation. Minerals Engineering 11, 1143-1160.
Kodali, P., Dhawan, N., Depci, T., Lin, C.L., Miller, J.D., 2011. Particle damage and exposure analysis in HPGR crushing of selected copper ores for column leaching. Minerals Engineering 24, 1478-1487.
Komar Kawatra, S., Carlson, J.T., 2014. Beneficiation of phosphate ore. Society for Mining, Metallurgy & Exploration.
Le Bas, M.J., Streckeisen, A.L., 1991. The IUGS systematics of igneous rocks. Journal of the Geological Society 148, 825-833.
Little, L., Mainza, A.N., Becker, M., Wiese, J.G., 2016. Using mineralogical and particle shape analysis to investigate enhanced mineral liberation through phase boundary fracture. Powder Technology 301, 794-804.
Maire, E., Withers, P.J., 2014. Quantitative X-ray tomography. International Materials Reviews 59, 1-43.
Mariano, R.A., Evans, C.L., Manlapig, E., 2016. Definition of random and non-random breakage in mineral liberation - A review. Minerals Engineering 94, 51-60.
Meloy, T.P., 1984. Liberation theory - Eight, modern, usable theorems. International Journal of Mineral Processing 13, 313–324.
Meloy, T.P., Preti, U., Ferrara, G., 1987. Liberation - Volume and mass lockedness profiles derived - Theoretical and practical conclusions. International Journal of Mineral Processing 20, 17-34.
Petruk, W., 1978. Correlation between grain sizes in polished section with sieving data and investigation of mineral liberation measurements from polished sections. Trans Inst Min Metall Sect C 87, c272-c277.
Rosiwal, A., 1898. Über geometrische Gesteinsanalysen. Jahrbuch der K. K. Geologischen Reichsanstalt, 143.
Sandmann, D., Gutzmer, J., 2013. Use of Mineral Liberation Analysis (MLA) in the Characterization of Lithium-Bearing Micas. Journal of Minerals and Materials Characterization and Engineering 01, 285-292.
Schranz, H., Berghöfer, W., 1958. Selektive Zerkleinerung. Bergb.-Wiss. 5, 8.
Singh, V., Venugopal, R., Banerjee, P.K., Saxena, V.K., 2014. Effect of morphology on breakage and liberation characteristics of minerals and coal. Minerals and Metallurgical Processing 31, 186-192.
Thomson, E., 1930. Quantitative Microscopic Analysis. The Journal of Geology 38, 29.
Veasey, T.J., Wills, B.A., 1991. Review of methods of improving mineral liberation. Minerals Engineering 4, 747-752.
Wills, B.A., Atkinson, K., 1993. Some observations on the fracture and liberation of mineral assemblies. Minerals Engineering 6, 697-706.
Xu, W., Dhawan, N., Lin, C.L., Miller, J.D., 2013. Further study of grain boundary fracture in the breakage of single multiphase particles using X-ray microtomography procedures. Minerals Engineering 46-47, 89-94.

ACCEPTED MANUSCRIPT

# Highlights

- grain boundary fracture was studied using MLA
- the amount of intergranular and transgranular fracture after grinding was measured
- the evolution of the percentage of detachment on liberation was studied with particle size
- different fracture and liberation characteristics are shown on 3 different materials

ACCEPTED MANUSCRIPT